bjh research paper

Proteomic profiling of naïve multiple myeloma patient plasma cells identifies pathways associated with favourable response to bortezomib-based treatment regimens

Dominik Dytfeld,[1,2] Shaun Rosebeck,[1] Malathi Kandarpa,[3] Anoop Mayampurath,[4] Dattatreya Mellacheruvu,[5,6] Mattina M. Alonge,[1] Lambert Ngoka,[7] Jagoda Jasielec,[1] Paul G. Richardson,[8] Samuel Volchenboum,[4] Alexey I. Nesvizhskii,[5] Arun Sreekumar[5,*] and Andrzej J. Jakubowiak[1]

[1]University of Chicago, Chicago, IL, USA, [2]Karol Marcinkowski University of Medical Sciences, Poznan, Poland, [3]Hematology/Oncology, University of Michigan Comprehensive Cancer Center, Ann Arbor, MI, [4]Center for Research Informatics, Computation Institute and Department of Pediatrics, University of Chicago, Chicago, IL, [5]Department of Pathology, University of Michigan, Ann Arbor, MI, [6]Department of Computational Medicine & Bioinformatics, Ann Arbor, MI, [7]Medical College of Georgia, Augusta, GA, and [8]Dana-Farber Cancer Institute, Boston, MA, USA

Received 26 November 2014; accepted for publication 4 February 2015
Correspondence: Andrzej J. Jakubowiak, University of Chicago, 5841 S. Maryland Ave, MC 2115, Chicago, IL 60637-6613, USA.
E-mail: ajakubowiak@medicine.bsd.uchicago.edu

*Present address: Department of Molecular and Cell Biology and Alkek Center for Molecular Discovery, Baylor College of Medicine, Houston, TX, USA

Summary

Toward our goal of personalized medicine, we comprehensively profiled pre-treatment malignant plasma cells from multiple myeloma patients and prospectively identified pathways predictive of favourable response to bortezomib-based treatment regimens. We utilized two complementary quantitative proteomics platforms to identify differentially-regulated proteins indicative of at least a very good partial response (VGPR) or complete response/near complete response (CR/nCR) to two treatment regimens containing either bortezomib, liposomal doxorubicin and dexamethasone (VDD), or lenalidomide, bortezomib and dexamethasone (RVD). Our results suggest enrichment of 'universal response' pathways that are common to both treatment regimens and are probable predictors of favourable response to bortezomib, including a subset of endoplasmic reticulum stress pathways. The data also implicate pathways unique to each regimen that may predict sensitivity to DNA-damaging agents, such as mitochondrial dysfunction, and immunomodulatory drugs, which was associated with acute phase response signalling. Overall, we identified patterns of tumour characteristics that may predict response to bortezomib-based regimens and their components. These results provide a rationale for further evaluation of the protein profiles identified herein for targeted selection of anti-myeloma therapy to increase the likelihood of improved treatment outcome of patients with newly-diagnosed myeloma.

Keywords: multiple myeloma, lenalidomide, bortezomib, proteomics.

The treatment of multiple myeloma (MM) has improved due to tremendous progress in recent years following the incorporation of immunomodulatory drugs, such as thalidomide, lenalidomide and pomalidomide, and proteasome inhibitors, including bortezomib and carfilzomib, into treatment strategies (Richardson *et al*, 2002, 2005; Dimopoulos *et al*, 2007; Harousseau *et al*, 2009; Dytfeld *et al*, 2011). Recently-introduced combination regimens using these novel agents show overall response rates of 90–100%, along with improved rates of very good partial response (VGPR) approaching 80%, complete and near complete response rates (CR/nCR) near 60% and stringent complete response (sCR) in up to 50% of patients (Harousseau & Moreau, 2009; Jakubowiak *et al*, 2012; Khan *et al*, 2012). With increasing rates of CR, evaluation of minimal residual disease (MRD) with a variety of techniques is now emerging as an additional measure of

First published online 30 March 2015
doi: 10.1111/bjh.13394

depth of response (Jakubowiak *et al*, 2012; Paiva *et al*, 2012). A number of studies have shown association between the depth of response (e.g. achievement of VGPR or CR/nCR to a given regimen or treatment strategy) and longer progression-free survival (PFS) and/or overall survival (OS) (Jakubowiak *et al*, 2009; Richardson *et al*, 2010; Khan *et al*, 2012). More recently, a similar positive association was reported for achieving MRD-negative status (Pineda-Roman *et al*, 2008; Paiva *et al*, 2012; Martinez-Lopez *et al*, 2014).

Observed differences in the degree of response to a given regimen may reflect variations in the biology of subsets of myeloma, underscoring the well-established heterogeneity of the disease within and between patients (Pineda-Roman *et al*, 2008; Harousseau *et al*, 2009; Cavo *et al*, 2010; Chanan-Khan & Giralt, 2010; Bolli *et al*, 2014; Lohr *et al*, 2014). In recognition of these differences, individualized approaches to treatment of subsets of myeloma or risk-adapted therapeutic strategies based on pre-treatment cytogenetics and/or gene expression profiling (GEP) have been proposed (Reece *et al*, 2009; Zhou *et al*, 2009; Mikhael *et al*, 2013). While these strategies address the treatment recommendations for patients with different risk factors, a truly individualized approach to myeloma patient therapy based on pre-treatment tumour characteristics that predicts very good response (e.g. VGPR or CR) and is statistically associated with improved time-to-event is lacking. Research in recent years has uncovered key targets and pathways involved in the response to the most common anti-myeloma agents, including cereblon as a target for immunomodulatory drugs (Zhu *et al*, 2011; Broyl *et al*, 2013; Gandhi *et al*, 2014), and TJP1 and XBP1 as markers of sensitivity to proteasome inhibitors (Leung-Hagesteijn *et al*, 2013; Zhang *et al*, 2013). These discoveries, along with characterization of new or previously unknown mutations associated with myeloma, such as mutations in *BRAF* (Chapman *et al*, 2011; Lohr *et al*, 2014), provide the opportunity for marker-based individualized therapy and for targeted selection of anti-myeloma agents to improve treatment outcome. However, translation of these discoveries into clinical practice is still in very early phases and more research is needed to advance precision medicine in myeloma.

Among various efforts to advance personalized therapy, proteomics-based techniques provide the opportunity to comprehensively interrogate the molecular heterogeneity of MM at the proteome level, which may in turn facilitate the implementation of marker-based individualized therapies (Unwin *et al*, 2006; Nicolas *et al*, 2011). Advanced quantitative proteomic technologies have been applied in studies of primary patient samples to identify biomarkers of disease and putative new targets for treatment and also to assist in the selection of initial therapy (Taguchi *et al*, 2007; Liang *et al*, 2012). Quantitative mass-spectrometry (MS)-based approaches, such as isobaric chemical labelling [e.g. isobaric tags for relative and absolute quantitation (iTRAQ)], are capable of accurate, precise and reproducible quantification and provide deep proteome coverage (Keshamouni *et al*, 2006). While several proteomic methodologies have been applied to basic research questions about MM biology and pathogenesis (reviewed in Cumova *et al*, 2011), there remains an unmet need for applying these technologies to the translation of protein-based biomarker discoveries into the clinic and thus improving and/or tailoring patient care.

In this paper, we present results from proteomic profiling of naive MM patient plasma cells (PC) to find patterns indicative of at least VGPR or CR/nCR to two treatment regimens: VDD (bortezomib, liposomal doxorubicin, dexamethasone) and RVD (lenalidomide, bortezomib, dexamethasone), respectively. Using complementary platforms of iTRAQ and label-free (LB) quantitative MS, and also GEP for VDD patients, we derived signatures associated with achievement of at least VGPR or CR/nCR to initial treatment and identified patterns of protein pathways associated with different levels of response to treatment with these two regimens.

Materials and methods

Myeloma patient samples and plasma cell enrichment

Bone marrow aspirates were obtained from 18 patients treated on a Phase II clinical trial with VDD (NCT00116961), and 16 patients enrolled at the University of Michigan site in the Phase II portion of the multi-site frontline clinical trial with RVD (NCT00378105). After approval by the site's Institutional Review Board, informed consent to treatment protocols and sample procurement was obtained for all cases included in this study. Details of both studies are described elsewhere (Jakubowiak *et al*, 2009; Richardson *et al*, 2010). Plasma cells (PC) from pre-treatment bone marrow aspirates were enriched by negative selection (RosetteSep® Multiple Myeloma enrichment cocktail, Stem Cell Technologies, Vancouver, BC, Canada) according to the manufacturer's recommendations. Pellets containing $0{\cdot}5 \times 10^6$ PC were flash frozen for storage. Only samples containing at least 80% PC purity, which was confirmed by Wright-Giemsa staining of post-enrichment cytospins, were further analysed.

Sample preparation for proteomics platforms

Isobaric tags for relative and absolute quantitation (iTRAQ). All reagents are from the iTRAQ 8-plex kit (Applied Biosystems, ThermoFisher Scientific, Waltham, MA, USA). Lysates from PC pellets were prepared according to the manufacturer's protocol. Each iTRAQ 8-plex experiment consisted of peptides from $0{\cdot}5 \times 10^6$ MM1.S cell lysates labelled with reagents 113 and 121 used as an internal control. Half of the remaining reagents were used to label samples from patients who achieved at least VGPR in the VDD portion of the study and

at least nCR for RVD, and the remaining half were used to label samples from patients with lesser response. The labelled peptide mixture was fractionated on a strong cation exchange (SCX) MicroSpin column with sequential elution of bound peptides. The eluate was dried and reconstituted in 0·1% trifluoroacetic acid (TFA) and then separated by reversed phase chromatography using a Zorbax 300 SB C18 column. Column effluent was mixed with matrix-assisted laser desorption/ionization (MALDI) matrix and spotted onto 192-well MALDI target plates that were later analysed by tandem MS. The MS and MS/MS spectra were acquired on an Applied Biosystems 4800 Proteomics Analyser [time-of-flight (TOF)/TOF; AB SCIEX, Framingham, MA, USA] in positive ion reflection mode. Single-stage mass spectra for all samples were collected first and in each sample well MS/MS spectra were acquired from the 12 most intense peaks above the signal-to-noise ratio threshold of 60. Protein identification and quantification were carried out using PROTEINPILOT software v2.0.1 (AB SCIEX) and the Celera protein sequence database (https://www.celera.com/), which comprises sequences from NCBI Refseq, Swiss-Prot, and TrEMBL databases. For assigning sequence identity, the Paragon algorithm was used (Shilov *et al*, 2007). All reported proteins were identified with a false discovery rate (FDR) <1% as determined by Paragon. Relative quantification of proteins was performed on the MS/MS scan using the area under the peaks at 113, 114, 115, 116, 117, 118, 119 and 121 Da, which are the masses of the tags corresponding to the iTRAQ reagents (Keshamouni *et al*, 2006). The peak areas of the iTRAQ reporters in each peptide were used to calculate ratios of patients (labels 114–119) versus the control MM1.S cell lysates used as reference for further analysis (Keshamouni *et al*, 2006). The reported ratios were automatically normalized using the applied bias factor obtained from the median ratio of all proteins that came from all the SCX fractions that were in each MS/MS run.

Label-free quantitation. Pellets containing $0{\cdot}5 \times 10^6$ PC from the same patients that were analysed by iTRAQ were lysed in radioimmunoprecipitation assay (RIPA) buffer (Pierce, ThermoFisher Scientific). Denatured samples were separated on 4–12% Bis-Tris gels (NuPAGE Novex; Invitrogen, ThermoFisher Scientific), which were stained with GelCode Blue (ThermoFisher Scientific). After each lane was cut into 22 equal pieces, gel plugs were de-stained with 30% methanol, washed with 25 mM ammonium bicarbonate in 50% acetonitrile (ACN), reduced with 10 mM dithiothreitol (ThermoFisher Scientific), alkylated using 50 mM iodoacetamide (Fluka Chemie, Sigma Aldrich Corporate, St. Louis, MO USA) and digested with trypsin (Sigma Aldrich Corporate). Peptides were extracted first with 0·1% TFA in 60% ACN and subsequently with 0·1% TFA in 100% ACN. Each supernatant was collected, pooled and dried, then reconstituted in solvent prior to liquid chromatography (LC)/MS analysis. Samples were analysed via liquid chromatography-electrospray ionization-tandem mass spectrometry (LC-ESI-MS/MS) on a linear ion trap mass spectrometer (LTQ; ThermoFisher Scientific) coupled to an Agilent Technologies (Santa Clara, CA, USA) nano LC system and a C18 reversed phase LC column (Micro-Tech Scientific, Orange, CA, USA). Data Dependent Analysis (DDA) mode was utilized on the LTQ to perform MS on all ions above an ion count of 1000.

Tandem MS spectra from the LTQ were searched with SEQUEST (http://fields.scripps.edu/sequest/index.html) against the human IPI protein database appended with an equal number of decoy (reversed) protein sequences (for FDR estimation). The output files were evaluated by PEPTIDEPROPHET (peptide-level analysis) and PROTEINPROPHET (protein inference) available as part of the Trans-Proteomic Pipeline (Deutsch *et al*, 2010). Protein identifications were filtered using the ProteinProphet-computed probability to achieve the FDR of <1% as estimated using the target-decoy strategy. Proteins were quantified using LF spectral counting strategy using ABACUS (Fermin *et al*, 2011).

Analysis of protein quantitation data

Proteomic signatures differentiating ≥VGPR from <VGPR for VDD and CR/nCR from <nCR for the RVD group were created from iTRAQ data as follows. First, the data was filtered by including only those proteins with acceptable control ratios (i.e. internal control MM1.S lysates with label 113:121 ≤ 1·5-fold change). Then, for each protein, the iTRAQ reporter ratios were averaged across patients in both responder and non-responder groups. The responder to non-responder expression ratios (i.e. (≥VGPR to <VGPR for VDD; CR/nCR to <nCR for RVD) were calculated in each of the three replicate datasets. Finally, these expression ratios for each protein were averaged across all replicates, which we denoted as the average protein expression ratio. The cut-off for differential expression was set at 1·5-fold, which is often used in proteomic studies (Ting *et al*, 2009). Figures S1 and S2 depicts the distribution of average ratios for proteins identified in VDD and RVD respectively, with line demarcations indicating proteins significant to responders in each treatment. Within the responder and non-responder groups, protein spectral counts were normalized by the total spectral count and averaged across patients. Protein fold change between responders and non-responders were calculated using these spectra counts and then were modelled as a Gaussian distribution. Figures S3 and S4 depicts the log-scale distribution of protein fold change in expression between responders and non-responders for VDD and RVD treatment regimen. Proteins on either side of a 2-standard deviation cut-off were selected as being significant to responders of VDD and RVD treatment. Figures S5 and S6 demonstrate the efficacy of data processing by comparing protein expression between LF and iTRAQ analysis for VDD and RVD, respectively.

RNA isolation and gene expression profiling (GEP)

Using Qiagen RNeasy minicolumns (Qiagen, Santa Clarita, CA, USA), total RNA was extracted from the PC of 18 patients enrolled in the VDD study. RNA quality was determined by assessing the presence of rRNA bands on an Agilent Bioanalyser (Agilent Technologies). When required, amplification of the transcriptome was performed using Ovation (Nugen Inc., San Carlos, CA, USA) to generate cDNA. cRNA was synthesized according to Affymetrix (Santa Clara, CA, USA) protocols and was labelled and hybridized to the U133plus 2·0 GeneChip, according to manufacturer's guidelines. The quality of the microarray data was analysed using a density plot of all perfect-match probes for each chip and degradation plot of the mean intensity for probes ordered according to where they bind to the mRNA transcript. A *t*-test was performed to identify 166 genes that were significantly different between ≥VGPR and <VGPR groups ($P < 0{\cdot}001$). Through permutation analysis using sample labels, an expected FDR of 24% was determined, and supported using Benjamini–Hochberg adjusted *P*-values. Log-rank tests for univariate association with VGPR were performed to generate heat map column dendrograms with hierarchical clustering.

Pathway analysis

Identified proteins were mapped to their corresponding gene symbols. Differentially expressed proteins in both LF and iTRAQ experimental groups are indicated by +1/−1 labels based on whether they were up- or down-regulated, with 0 label indicating proteins whose expression were unchanged between analysed groups. Within RVD and VDD, the iTRAQ and LF lists were combined as follows: Proteins with consistent labels in both lists were retained. Additionally, proteins with differential label (+1/−1) in one list but with a 0 or missing label in the other list were retained. Proteins with inconsistent labels (i.e. +1 in one list, −1 in the other) were ignored. Signature proteins (i.e. mapped gene symbols) and their labels were used as input to the Ingenuity Pathway Analysis software (IPA; Qiagen). Ingenuity Pathway Analysis encompasses the Ingenuity Pathway Analysis Knowledge Base (IPA KB, http://www.ingenuity.com/), a hand-curated database of all published protein interactions. Here, a given signature gene list was mapped to IPA KB with labels being denoted as 'Other' within the analysis. Default parameters were used and species was selected as human. Pathway analysis was conducted separately for RVD and VDD groups, following which a comparison analysis was made between them. Fisher's exact test was used to calculate *P*-values for determining significance of overlap between the proteins in each dataset and the canonical pathways within IPA KB. Additionally for each analysis, IPA software was used to generate hypothetical networks from the list of molecules (called focus genes) and score them based on log-scale *P*-values indicative of the probability of including a gene in a network purely by random chance.

Similarly to proteomics analysis, the 166 differential genes from the GEP data from VDD patients were labelled as +1/−1, following which the IPA-determined pathways were compared to corresponding VDD protein signatures.

Results

Proteomic analysis of patients enrolled in VDD study

The clinical characteristics of the 18 patients used in this analysis (Table I), were generally comparable to all 40 patients treated with VDD in the phase II trial (Jakubowiak *et al*, 2009), with the single exception of higher representation of patients with deletion of chromosome 13 in the ≥VGPR group (data not shown). Response rates and survival, including survival based on level of response to 6 weeks of VDD, were previously reported (Jakubowiak *et al*, 2009; Dytfeld *et al*, 2011). This time point was selected as a surrogate endpoint for prediction of PFS, regardless of level of response in later stages of treatment.

A total of 944 proteins were detected from the iTRAQ experiments, while the LF approach yielded 900 proteins, with 512 proteins in common between both methods (Fig 1A, FDR <1%). Among the 356 differentially expressed proteins detected from iTRAQ analysis, 195 were up-regulated and 161 were down-regulated in samples from patients achieving ≥VGPR. From the LF analysis, 90 proteins (40 proteins up-regulated and 50 down-regulated in the ≥VGPR group) were differentially expressed. In LF method, the strict definition of differential expression in the data (top and bottom 5% after Gaussian fitting) resulted in assigning no change to most proteins and only a small overlap of differentially expressed proteins between the two platforms (not shown), which is in agreement with previous work (Vellaichamy *et al*, 2009).

Table I. Clinical characteristics of patients treated with RVD and VDD profiled in this analysis.

Clinical characteristic	VDD ($n = 18$)	RVD ($n = 16$)
Median age, years (range)	57 (44–74)	60 (43–82)
Sex ratio (male/female)	12/6	8/8
Salmon-Durie stage I/II/III	1/5/12	3/4/9
ISS stage1/2/3	5/5/8	7/6/3
Cytogenetics (SR/HR)	11/7	8/8
Best response (CR/nCR/VGPR/PR/PD)	2/1/7/8/0	4/4/5/3/0
Alive/Dead	14/4	12/4
Not progressed/Progressed	12/6	10/6

RVD, lenalidomide, bortezomib, dexamethasone; VDD, bortezomib, liposomal doxorubicin, dexamethasone; ISS, International staging system; SR, standard risk; HR, high risk; CR, complete response; nCR, near complete response; VGPR, very good partial response; PR, partial response; PD, progressive disease.

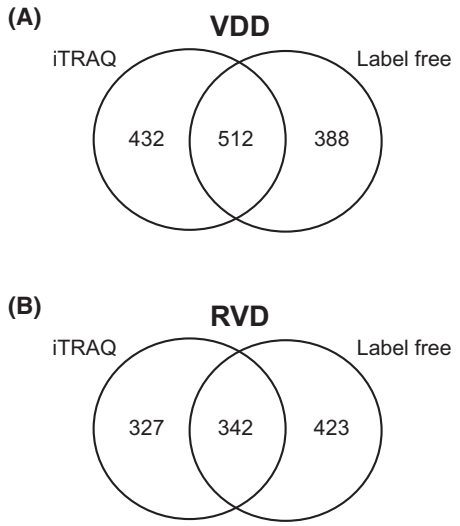

Fig 1. Proteomic analysis of samples from VDD (A) and RVD (B) cohorts. Protein IDs were mapped to gene symbols and tabulated. (A) Comparison of protein identification using both LF and iTRAQ on all VDD samples based on achieving at least very good partial response (VGPR) or better vs. less than VGPR. (B) Comparison of protein identification using both LF and iTRAQ on all RVD samples based on achieving near-complete response/complete response (CR) versus less than CR. RVD, lenalidomide, bortezomib, dexamethasone; VDD, bortezomib, liposomal doxorubicin, dexamethasone; LF, Label-free quantitation; iTRAQ, isobaric tags for relative and absolute quantitation

Proteomic analysis of patients treated with RVD

Analysis was performed on 16 patients (Table I) treated with the RVD regimen and was based on whether or not patients achieved CR/nCR after six cycles of RVD, a prognostic indicator of higher significance than VGPR. The response rates and survival in the RVD trial have been previously reported (Richardson *et al*, 2010).

Based on iTRAQ analysis, a total of 669 proteins were detected (Fig 1B, FDR <1%). Comparison of proteomic alterations in CR/nCR vs. a lesser response in the RVD cohort of patients revealed the up-regulation of 161 proteins, while 98 proteins showed reduced expression in iTRAQ analysis. The LF approach yielded 765 proteins (Fig 1B, FDR <1%), of which 40 proteins were up-regulated, while 31 proteins were down-regulated in patient samples associated with nCR/CR response. Similar to the VDD study, the LF approach in RVD also demonstrated that a majority of proteins remain unchanged (top and bottom 5% after Gaussian fitting).

Network analysis of differentially expressed proteins in VDD and RVD

To understand molecular variations between different levels of response among the two drug regimens, analysis was performed at the pathway level on both cohorts of samples. In VDD-treated patients, 211 proteins were up-regulated and 195 down-regulated among those that were mapped to the IPA KB database after merging the iTRAQ and LF protein lists (with 27 proteins unmapped). The complete list of mapped and un-mapped proteins (given as gene symbols) along with assigned labels is given in Table SI. Figure 2A depicts the top ten canonical pathways (based on the log of the p-value from Fisher's exact test) identified in the cohort of patients achieving at least VGPR on the VDD regimen, of which mitochondrial dysfunction (*P*-value: $1{\cdot}44^{-09}$), oxidative phosphorylation (*P*-value: $2{\cdot}00^{-08}$), and EIF2 signalling (*P*-value: $2{\cdot}37^{-08}$) are most confidently associated. Networks of proteins with overlaying canonical pathways were generated for the VDD proteomic profile, and the one with the highest score (46) had 32 network-seeding focus molecules and was most closely associated with cell death and survival (IPA reported *P*-value: $3{\cdot}40^{-07}$, Figure S7).

In RVD-treated patients, 316 differential proteins were identified from merging iTRAQ and LF protein lists, of which 292 were successfully mapped to the IPA KB. Out of this set, 178 proteins were up-regulated and 114 proteins were down-regulated in the nCR/CR group (Table SII). As in the VDD-treated patients, EIF2 signalling is among the top canonical pathways (*P*-value: $3{\cdot}17^{-12}$) enriched by proteins from the signature differentiating patients who achieved at least nCR in response to RVD (Fig 2B). Other high-scoring networks include liver X receptor/retinoid X receptor (LXR/RXR) activation (*P*-value: $2{\cdot}17^{-07}$) and remodelling of epithelial adherens junctions (*P*-value: $2{\cdot}19^{-07}$). The IPA-generated network with the highest score (48) had 31 focus molecules and was associated most closely with RNA post-transcriptional modification (*P*-value = $1{\cdot}95^{-08}$, Figure S8). Also shown in Figure S2 is the overlap of this network with the four major canonical pathways identified in Fig 2B.

Using the IPA comparative analysis mode, a comparison of pathways generated from VDD responders (≥VGPR) was made with those identified in RVD responders (CR/nCR. Figure 3A depicts the top common and unique pathways between cohorts. As shown earlier, differential EIF2 signalling was found in common and with high confidence scores in both VDD and RVD. Other high-scoring common differential pathways include remodelling of epithelial adherens junctions, clathrin-mediated endocytosis signalling, epithelial adherens junction signalling and actin cytoskeleton signalling. Among the differential pathways, mitochondrial dysfunction was found to be significant in VDD ($P < 0{\cdot}05$) in contrast with RVD. Figure 3B shows the oxidative phosphorylation pathway, a subset of mitochondrial dysfunction, for both VDD and RVD signature proteins. As can be seen, the presence of NADH dehydrogenase class of proteins in the VDD signature profile results in a higher enrichment of this pathway in the VDD cohort.

GEP of patients treated with VDD

A subset of 24 patients treated with VDD with available RNA from isolated PC was analysed for GEP using the

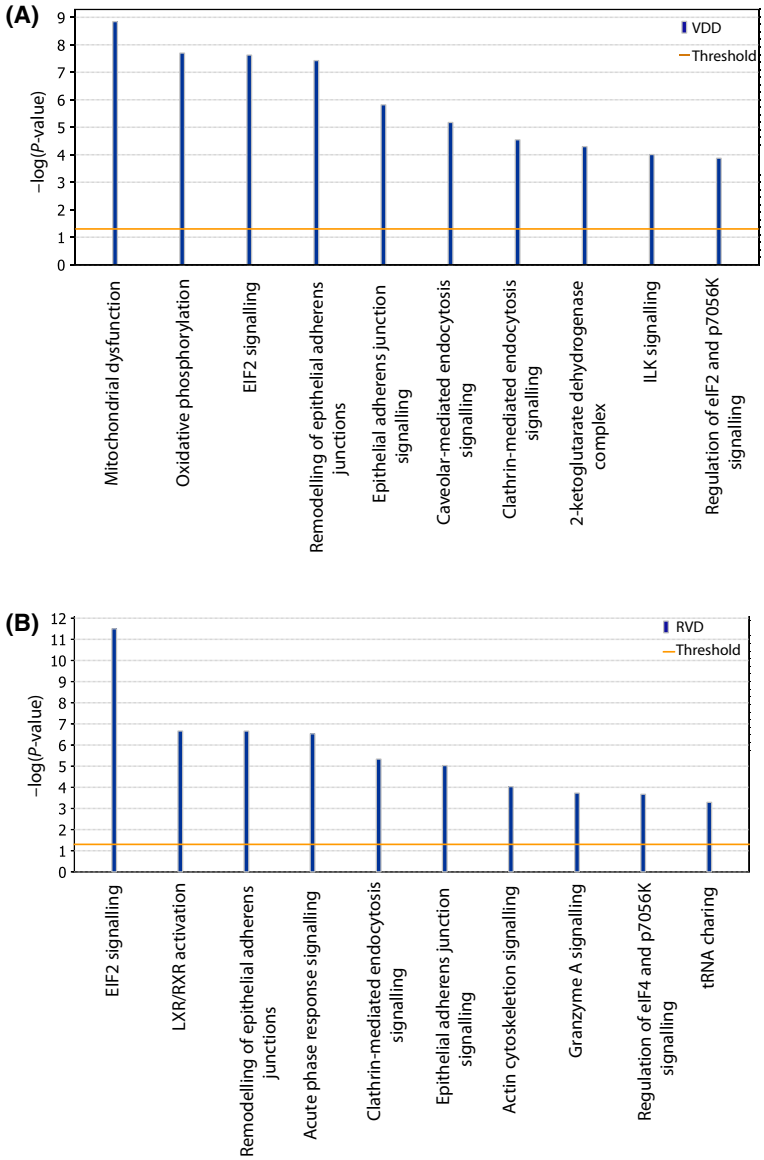

Fig 2. Proteomic profiling of differential proteins in VDD and RVD studies. (A) A list of the top ten canonical pathways identified to be dominant from the Ingenuity Pathway Analysis (IPA) of differential proteins indicative of favourable response to VDD. The threshold is marked for a *P*-value of 0·05. Mitochondrial dysfunction, oxidative phosphorylation and EIF2 signalling are identified with most confidence. (B) A list of top ten canonical pathways identified to be dominant from the IPA analysis of differential proteins identified in the cohort of RVD patients who achieved near-complete response/complete response. Threshold is marked for *P*-value of 0·05. EIF2 signalling, LXR/RXR activation, remodelling of epithelial adherens junctions, and acute phase response signalling were identified with most confidence. RVD, lenalidomide, bortezomib, dexamethasone; VDD, bortezomib, liposomal doxorubicin, dexamethasone.

Affymetrix U133plus 2·0 GeneChip. Twenty of these samples passed RNA quality control and 18 samples were evaluable after GEP analysis, nine from patients achieving ≥VGPR and nine from patients achieving <VGPR. Of this group, eight patients were among those subjected to proteomic analysis. The GEP signature demonstrated 166 genes differentially regulated in patients based on whether or not VGPR was achieved in response to VDD therapy (Fig 4). The top 20 differentially up- and down-regulated genes in VDD ≥VGPR responders are highlighted. Ingenuity Pathway Analysis of our GEP signature identified oxidative phosphorylation as the predominant pathway enriched among responders. In comparison with the VDD GEP data, it was noted that the COX class of proteins that form Complex IV is up-regulated at the genome level, but down-regulated at the proteome level (Fig 5).

Discussion

With recognition of the heterogeneity of MM, there is an increasing interest in improving treatment using individualized therapy based on pre-treatment disease characteristics and/or biomarkers. In this report, we describe the novel application of two independent proteomic techniques to identify pre-treatment expression patterns in malignant PC indicative of response to initial treatment with VDD and RVD. We and others have reported that depth of response may serve as a surrogate for final endpoints, including PFS and OS (Dytfeld *et al*, 2011). Therefore, we used early response criteria, i.e. achievement of VGPR or CR within six cycles of treatment, as a predictor of clinical outcome.

The use of multiple proteomic platforms can greatly expand the sensitivity of observed differences in protein

expression and improve the probability of establishing a proteomic signature of response to treatment. Through a combined analysis of PC samples on iTRAQ and LF platforms, we identified 406 proteins in VDD patients who achieved at least VGPR versus those with lower response, and 292 proteins differentiating patients who achieved at least nCR versus those with lower response to RVD treatment. Although comparative proteomics is a powerful analytical method for learning the biology of the cell, considerable issues remain, such as incomplete proteome coverage and variations in quantitation values for specific proteins both within and across different platform MS runs. In addition, we applied stringent statistical analyses in the LF method by including only the top and bottom 5% of all identified differentially expressed proteins after Gaussian fitting. This resulted in only modest overlap of identified proteins between LF and iTRAQ (38% in the VDD study and 31% in the RVD). This is comparable to similar published data (Usaite *et al*, 2008; Patel *et al*, 2009), and is a widely recognized limitation of proteomic methods (Chandramouli & Qian, 2009; Wang *et al*, 2012). An optimal approach to comprehensive analysis has not yet been established and studies comparing different quantitative proteomics platforms are lacking. We approached the limitations in identification of a consensus list of differentially expressed proteins by performing pathway analyses and comparing the profiles of PC from patients treated with RVD and VDD based on response. This approach allowed us to consider groups of proteins rather than individual proteins alone to predict response and identify statistical differences in patterns associated with response to two treatment regimens, despite a relatively small number of samples available for analysis.

Pathway analysis of proteomic profiles of responders to both RVD and VDD therapy depicted a number of pathways not only specific to each drug regimen but also in common to both. For example, our study highlighted the endoplasmic reticulum (ER) stress response, more specifically EIF2 signalling, as the most prominent pathway associated with patients that responded best to both regimens (i.e. ≥VGPR on VDD or CR/nCR on RVD). Because MM PC produce large amounts of immunoglobulins, they operate with an elevated demand on the ER and are known to exhibit constitutive activation of ER stress pathways (Obeng *et al*, 2006), which function to halt most protein translation, increase expression of ER chaperones and, under conditions of extreme or prolonged stress, induce apoptotic effectors. Interestingly, it is this very nature of MM PC that renders them more susceptible to proteasome inhibition, which induces extreme stress in the ER and promotes apoptosis. Both drug regimens under examination in our multi-platform proteomic profiling of MM PC contain the proteasome inhibitor bortezomib. Our data suggest that, although MM PC require basal ER stress for optimal survival in the setting of increased metabolic demands, a threshold of ER stress response-associated proteins may need to be crossed in order to exhibit an optimal response to proteasome inhibitor-based regimens. Indeed, it has been reported that the degree of EIF2 phosphorylation itself, a key determinant in the outcome of ER stress, may be responsible for resistance to bortezomib (Schewe & Aguirre-Ghiso, 2009), suggesting that, in patients who did not respond well in our completed trials (i.e. <VGPR on VDD or <nCR), ER stress responses are somehow attenuated. In addition, the EIF2 pathway was recently highlighted as a critical determinant of dexamethasone-induced apoptosis in MM cells (Burwick *et al*, 2013). Taken together, our results suggest that detection of enriched EIF2

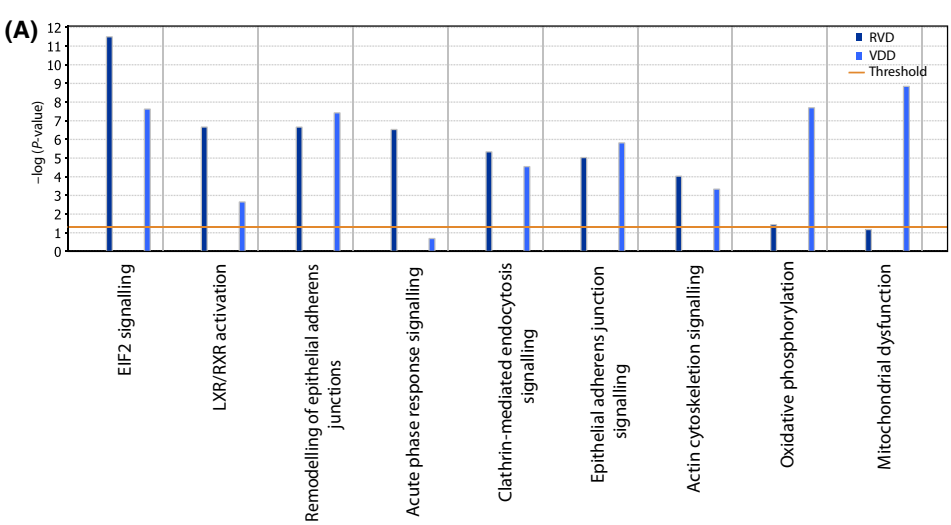

Fig 3. Comparison of pathways between VDD and RVD. (A) EIF2 signalling, LXR/RXR activation, remodelling of epithelial adherens junctions, clathrin-mediated endocytosis, and actin cytoskeleton signalling are pathways common to both RVD and VDD. Mitochondrial dysfunction was significantly more prevalent in VDD than RVD. On the other hand, Acute Phase Response signalling and was more prevalent in RVD. (B) Red depicts up-regulated and green depicts down-regulated. In VDD, Complex-I (NADH Dehydrogenase) is seen to be active along with a down-regulation of cytochrome c. RVD, lenalidomide, bortezomib, dexamethasone; VDD, bortezomib, liposomal doxorubicin, dexamethasone.

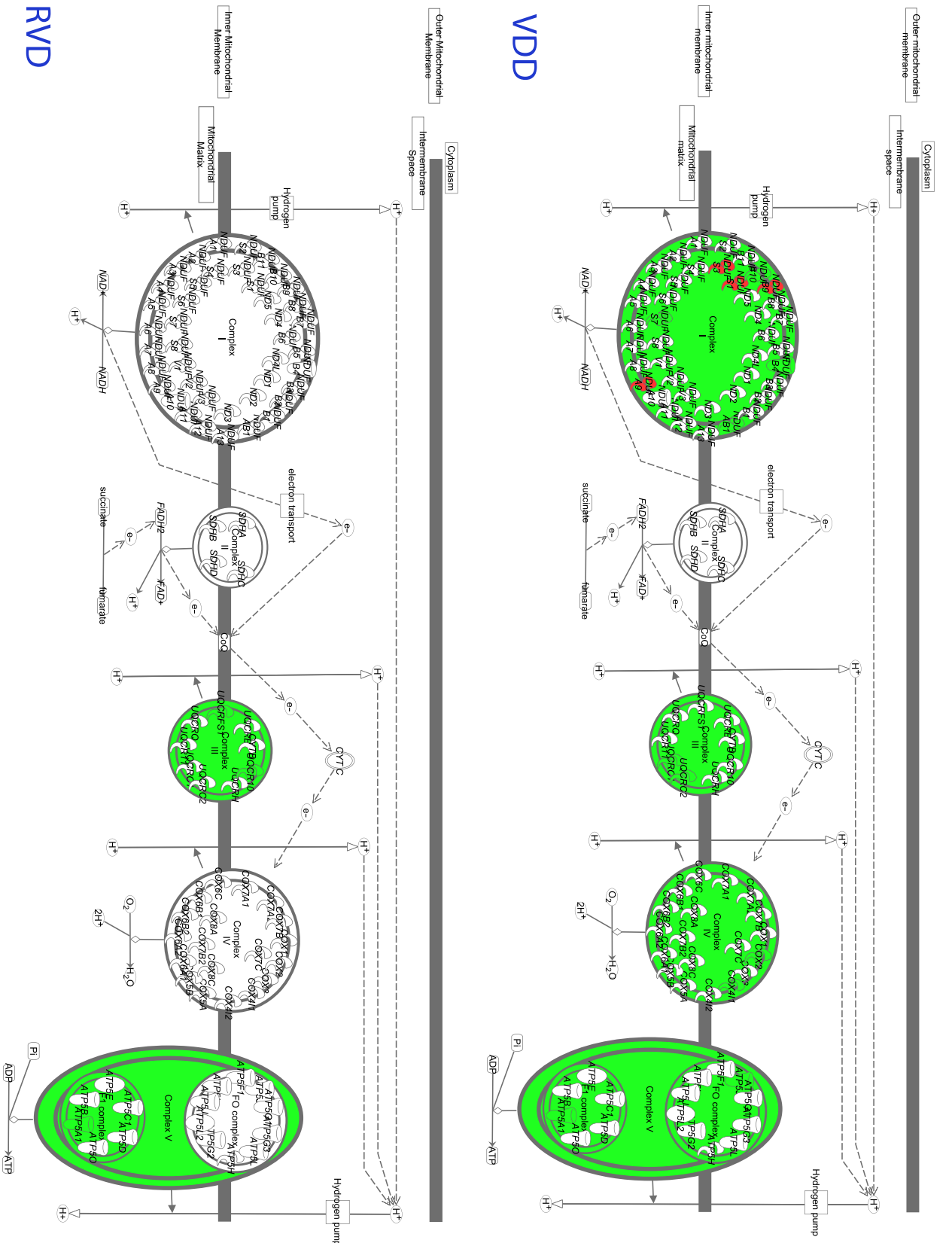

Fig 3. Continued.

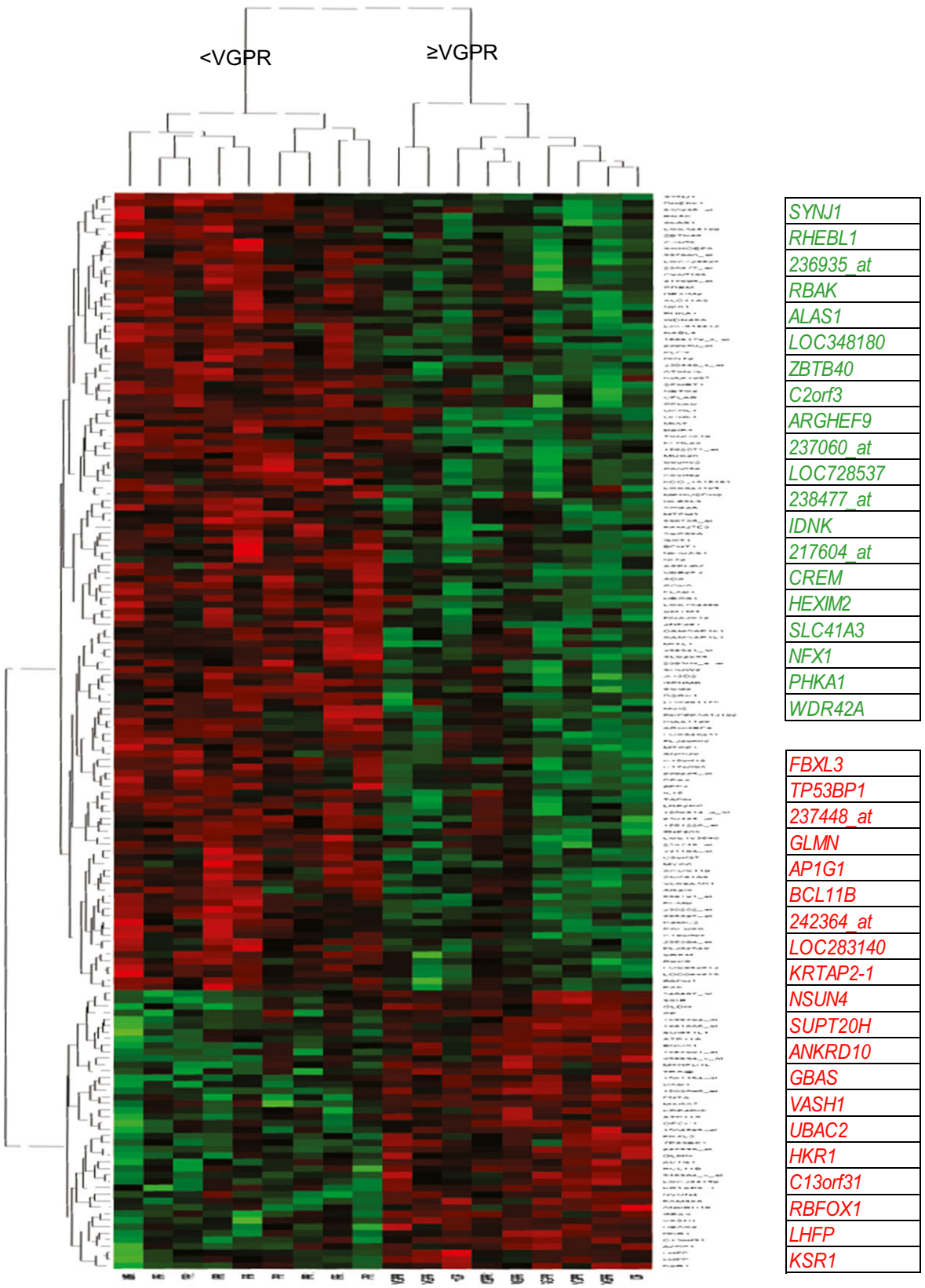

Fig 4. Gene expression profiling on VDD samples. Gene expression profiling correlation with VDD response in terms of achieving at least VGPR. The top 20 probe sets/genes increased in those achieving VGPR or better are highlighted in green and the top 20 probe sets/genes decreased in the same group are highlighted in red. VDD, bortezomib, liposomal doxorubicin, dexamethasone; VGPR, very good partial response.

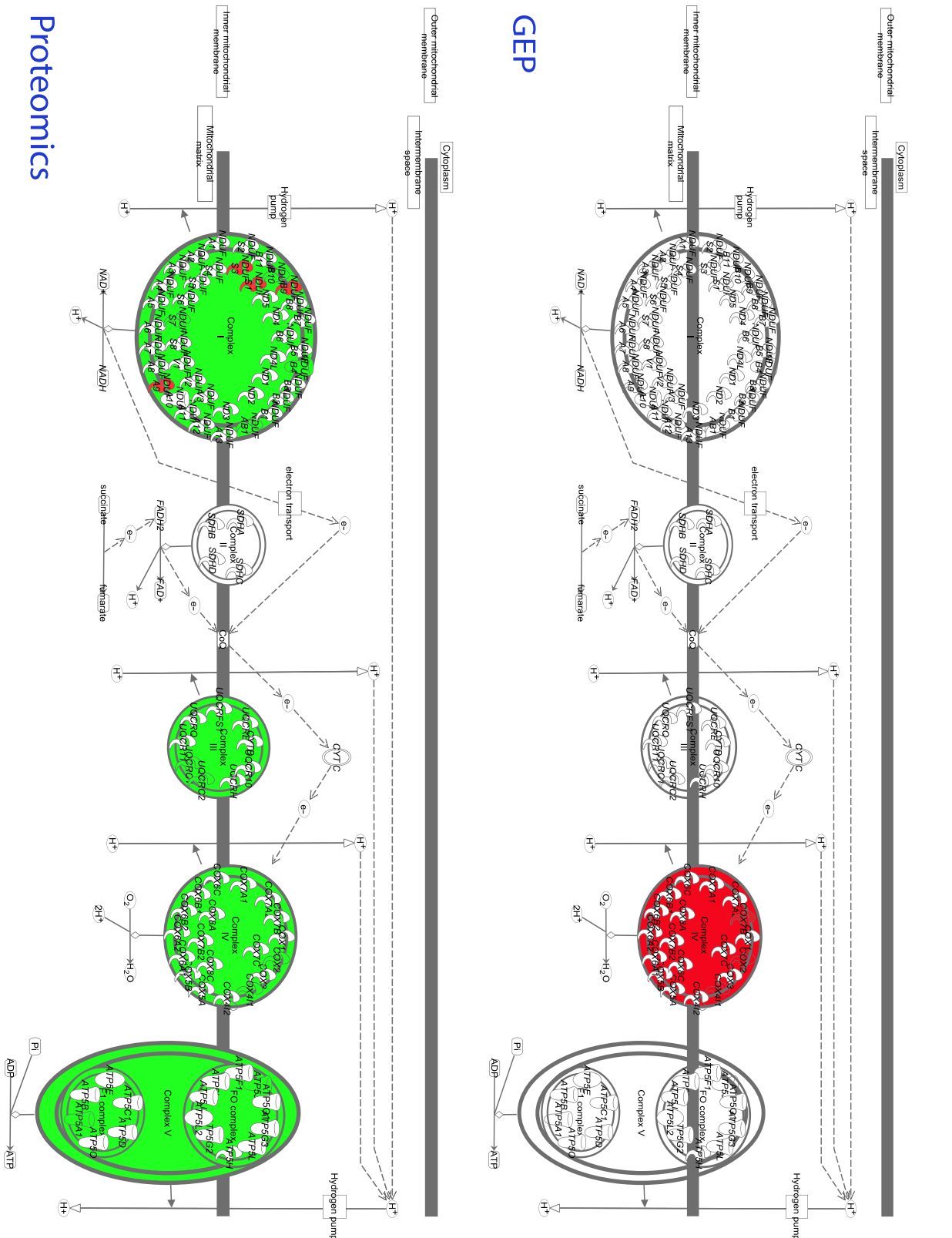

Fig 5. Comparison of oxidative phosphorylation pathway between GEP and protein signatures in VDD. Oxidative phosphorylation pathway comparison of the VDD GEP signature against the differential protein labels in VDD datasets revealed up-regulation of Complex IV (cytochrome c oxidase) in the GEP dataset as opposed to down-regulation in the proteomics dataset. VDD, bortezomib, liposomal doxorubicin, dexamethasone; GEP, gene expression profiling.

signalling-associated proteins in pre-treatment MM PC may serve as a useful 'universal response pathway' and predictive marker of positive response in newly-diagnosed MM patients treated with a regimen that includes bortezomib and dexamethasone.

Although EIF2 signalling was associated with those patients responding well to both RVD and VDD treatment, other pathways were found to be uniquely differentially regulated in each regimen. The proteomic signature predicting achievement of ≥VGPR to initial treatment with VDD revealed mitochondrial dysfunction as the top-ranked canonical pathway, which was not differentially expressed according to outcome in the RVD cohort. Interestingly, a common phenomenon associated with deregulated cancer cell proliferation is the corresponding alteration in energy metabolism, which is classically viewed as mitochondrial dysfunction (reviewed in Ward & Thompson, 2012). Furthermore, changes in expression of specific metabolic enzymes have been associated with sensitivity to genotoxic stimuli. Indeed, it has been demonstrated that decreased expression of a NADH dehydrogenase subunit is associated with resistance to doxorubicin (Wong *et al*, 2000). Accordingly, patients achieving better response to VDD demonstrate an enrichment of these proteins. In addition, enhanced production of reactive oxygen species (ROS) has also been shown to sensitize transformed cells to the effects of genotoxic stress (Benhar *et al*, 2001). Our results suggest that in MM PC, modulation of enzymes that can elevate ROS in the setting of altered mitochondrial function will provide a therapeutic benefit to those patients receiving a DNA-damaging agent, such as doxorubicin. In patients treated with RVD, a regimen in which the thalidomide derivative, lenalidomide, is used in combination with bortezomib and dexamethasone instead of doxorubicin (as in VDD), enrichment of the Acute Phase Response Signalling pathway is associated with better response. The predominant cytokine associated with the Acute Phase Response is IL6, an essential myeloma cell survival factor. The mechanism of action of immunomodulatory drugs, such as lenalidomide, is to inhibit production of pro-inflammatory cytokines, including TNF (also termed TNFα), IL1B, and IL6, and to co-stimulate T-cells and natural killer cells to elicit tumouricidal activity (Richardson *et al*, 2002). It stands to reason that a group of patients with an enriched signature of Acute Phase Response cytokines would benefit from a regimen containing an immune modulating compound, as demonstrated by our cohort of best responders among patients treated with RVD.

Altogether, our findings highlight dysregulated, therapeutically-relevant pathways that are of biological significance to MM. Furthermore, these studies lay the groundwork for the application of high-resolution quantitative proteomics to personalizing treatment options for newly-diagnosed MM patients. However, prospective validation of these techniques on a larger cohort of patients is required. Indeed, and as mentioned above, one potential drawback of our study is the limited number of samples in our training sets, i.e. the number of samples derived from patients enrolled in both VDD and RVD clinical trials, even if we are confident in our findings and in the stringency of our statistical analyses. With this in mind, we are currently prospectively collecting patient samples from additional trials already in progress, including two with bortezomib-based regimens and one with carfilzomib-based regimen, with the correlative objectives to perform much needed validation analyses based on findings from this report.

As GEP is more widely used for analysis of myeloma samples, we performed an exploratory comparison of the results between proteomic platforms and GEP on our VDD samples. The analysis revealed that all but six of the differentially expressed genes in our 166-gene GEP model were different from the proteins identified as differentially expressed in our proteomic signatures (data not shown). Furthermore, using IPA to compare oxidative phosphorylation, which was the only pathway subset enriched at both the proteomic and genomic level in patients achieving VGPR or better on the VDD regimen, showed opposite trends. While GEP highlighted up-regulation of complex IV-associated genes, proteomic evaluation of this subset demonstrated down-regulation. While potentially worrisome, overall, these results are in line with the well-recognized phenomenon of limited concordance between GEP and protein levels, and further support efforts made at interrogating the more biologically-relevant proteome level (De Wit *et al*, 2010; Vogel *et al*, 2010; Schwanhausser *et al*, 2011). This is reinforced by the discovery of novel protein pathway biomarkers, which our results suggest may be relevant as predictors of response to bortezomib-based therapeutic regimens. However, we recognize that more work is necessary to determine the applicability of these pathway-based biomarkers as a tool to bridge the gap between these translational bench-based observations and deployment in the clinic.

In summary, profiling of patient samples collected prior to treatment with VDD and RVD showed, as a proof of concept, that it is possible to identify proteomic patterns specific to response and treatment outcome. We believe that these results may represent the first proteomic-based step in a broader effort to establish marker-based personalized approaches for the selection of treatment in MM. The predictive capabilities of these patterns, along with applicability to therapeutic guidance need to be explored further.

Acknowledgements

The authors would like to thank Diane Durecki and Kathryn McDonnell for their assistance with clinical data collection.

Financial support: This study was supported by grants to A.S. and A.J.J. from the Multiple Myeloma Research Foundation and the Leukemia and Lymphoma Society. D.D. received a research grant from Janssen-Cilag.

Author contributions

D.D., M.K., A.I.N., A.S., and A.J.J. designed and performed the research study; L.N. and P.G.R. contributed essential

reagents and tools to complete the study; D.D., S.R., M.K., A.M., D.M., M.M.A., L.N., J.J., P.G.R., S.V., A.I.N., A.S., and A.J.J. took part in data acquisition, analysis, and interpretation; D.D., S.R., M.K., A.M., D.M., M.M.A., J.J., P.G.R., S.V., A.I.N., A.S., and A.J.J. wrote, reviewed, and/or revised the manuscript; D.D., S.R., M.K., A.M., D.M., M.M.A., L.N., J.J., P.G.R., S.V., A.I.N., A.S., and A.J.J. approved the final version of the manuscript.

Conflict of interest

A.J.J. is a consultant and member of the speakers bureau and advisory board for Millennium Pharmaceuticals, Inc., Celgene, and Janssen-Cilag, and has received honoraria from Millennium Pharmaceuticals, Inc., Celgene, Janssen-Cilag, and Takeda. D.D. has received honoraria from Janssen-Cilag. The remaining authors declare no competing financial interests.

Supporting Information

Additional Supporting Information may be found in the online version of this article:

Fig S1. Detection of proteins significant to responders in VDD using iTRAQ.

Fig S2. Detection of proteins significant to responders in RVD using iTRAQ.

Fig S3. The ratio of normalized spectrum counts from VDD samples was calculated and then log-transformed.

Fig S4 The ratio of normalized spectrum counts from RVD samples was calculated and then log-transformed.

Fig S5. Protein expression comparison between LF and iTRAQ experiment in VDD patient samples.

Fig S6. Protein expression comparison between LF and iTRAQ experiment in RVD patient samples.

Fig S7. Highest scoring network for VDD signature proteins.

Fig S8. Highest scoring network generated for RVD signature proteins.

Table SI. Proteins differentially regulated between responders and non responders to VDD (both iTRAQ and LF) successfully mapped to IPA KB.

Table SII. Proteins differentially regulated between responders and non responders to RVD (both iTRAQ and LF) successfully mapped to IPA KB.

References

Benhar, M., Dalyot, I., Engelberg, D. & Levitzki, A. (2001) Enhanced ROS production in oncogenically transformed cells potentiates c-Jun N-terminal kinase and p38 mitogen-activated protein kinase activation and sensitization to genotoxic stress. *Molecular and Cellular Biology*, **21**, 6913–6926.

Bolli, N., Avet-Loiseau, H., Wedge, D.C., Van Loo, P., Alexandrov, L.B., Martincorena, I., Dawson, K.J., Iorio, F., Nik-Zainal, S., Bignell, G.R., Hinton, J.W., Li, Y., Tubio, J.M.C., McLaren, S., O' Meara, S., Butler, A.P., Teague, J.W., Mudie, L., Anderson, E., Rashid, N., Tai, Y-T, Shammas, M.A., Sperling, A.S., Fulciniti, M., Richardson, P.G., Parmigiani, G., Magrangeas, F., Minvielle, S., Moreau, P., Attal, M., Facon, T., Futreal, P.A., Anderson, K.C., Campbell, P.J. & Munshi, N.C. (2014). Heterogeneity of genomic evolution and mutational profiles in multiple myeloma. *Nature Communications* **5**, doi:10.1038/ncomms3997.

Broyl, A., Kuiper, R., van Duin, M., van der Holt, B., el Jarari, L., Bertsch, U., Zweegman, S., Buijs, A., Hose, D., Lokhorst, H.M., Goldschmidt, H., Sonneveld, P., Hg, D-B & German, G.G. (2013) High cereblon expression is associated with better survival in patients with newly diagnosed multiple myeloma treated with thalidomide maintenance. *Blood*, **121**, 624–627.

Burwick, N., Delrow, J.J. & Shimamura, A. (2013) Translational profiling reveals the eIF2 kinase pathway as a mediator of dexamethasone induced apoptosis in multiple myeloma. *Blood* (ASH Annual Meeting Abstracts), **122**, 3104.

Cavo, M., Tacchetti, P., Patriarca, F., Petrucci, M.T., Pantani, L., Galli, M., Di Raimondo, F., Crippa, C., Zamagni, E., Palumbo, A., Offidani, M., Corradini, P., Narni, F., Spadano, A., Pescosta, N., Deliliers, G.L., Ledda, A., Cellini, C., Caravita, T., Tosi, P. & Baccarani, M. (2010) Bortezomib with thalidomide plus dexamethasone compared with thalidomide plus dexamethasone as induction therapy before, and consolidation therapy after, double autologous stem-cell transplantation in newly diagnosed multiple myeloma: a randomised phase 3 study. *Lancet*, **376**, 2075–2085.

Chanan-Khan, A.A. & Giralt, S. (2010) Importance of achieving a complete response in multiple myeloma, and the impact of novel agents. *Journal of Clinical Oncology: Official Journal of the American Society of Clinical Oncology*, **28**, 2612–2624.

Chandramouli, K, Qian, PY (2009). Proteomics: challenges, techniques and possibilities to overcome biological sample complexity. *Human Genomics and Proteomics: HGP*, **2009**, Dec 8;2009. pii: 239204. doi: 10.4061/2009/239204

Chapman, M.A., Lawrence, M.S., Keats, J.J., Cibulskis, K., Sougnez, C., Schinzel, A.C., Harview, C.L., Brunet, J.-P., Ahmann, G.J., Adli, M., Anderson, K.C., Ardlie, K.G., Auclair, D., Baker, A., Bergsagel, P.L., Bernstein, B.E., Drier, Y., Fonseca, R., Gabriel, S.B., Hofmeister, C.C., Jagannath, S., Jakubowiak, A.J., Krishnan, A., Levy, J., Liefeld, T., Lonial, S., Mahan, S., Mfuko, B., Monti, S., Perkins, L.M., Onofrio, R., Pugh, T.J., Rajkumar, S.V., Ramos, A.H., Siegel, D.S., Sivachenko, A., Stewart, A.K., Trudel, S., Vij, R., Voet, D., Winckler, W., Zimmerman, T., Carpten, J., Trent, J., Hahn, W.C., Garraway, L.A., Meyerson, M., Lander, E.S., Getz, G. & Golub, T.R. (2011) Initial genome sequencing and analysis of multiple myeloma. *Nature*, **471**, 467–472.

Cumova, J., Potacova, A., Zdrahal, Z. & Hajek, R. (2011) Proteomic analysis in multiple myeloma research. *Molecular Biotechnology*, **47**, 83–93.

De Wit, M., Keil, D., van der Ven, K., Vandamme, S., Witters, E. & De Coen, W. (2010) An integrated transcriptomic and proteomic approach characterizing estrogenic and metabolic effects of 17 alpha-ethinylestradiol in zebrafish (Danio rerio). *General and Comparative Endocrinology*, **167**, 190–201.

Deutsch, E.W., Mendoza, L., Shteynberg, D., Farrah, T., Lam, H., Tasman, N., Sun, Z., Nilsson, E., Pratt, B., Prazen, B., Eng, J.K., Martin, D.B., Nesvizhskii, A.I. & Aebersold, R. (2010) A guided tour of the Trans-Proteomic Pipeline. *Proteomics*, **10**, 1150–1159.

Dimopoulos, M., Spencer, A., Attal, M., Prince, H.M., Harousseau, J.L., Dmoszynska, A., San Miguel, J., Hellmann, A., Facon, T., Foa, R., Corso, A., Masliak, Z., Olesnyckyj, M., Yu, Z., Patin, J., Zeldis, J.B. & Knight, R.D. (2007) Lenalidomide plus dexamethasone for relapsed or refractory multiple myeloma. *The New England Journal of Medicine*, **357**, 2123–2132.

Dytfeld, D., Griffith, K.A., Friedman, J., Lebovic, D., Harvey, C., Kaminski, M.S. & Jakubowiak, A.J. (2011) Superior overall survival of patients with myeloma achieving very good partial response or better to initial treatment with bortezomib, pegylated liposomal doxorubicin, and dexamethasone, predicted after two cycles by a free light chain- and M-protein-based model:

extended follow-up of a phase II trial. *Leukaemia & Lymphoma*, **52**, 1271–1280.

Fermin, D., Basrur, V., Yocum, A.K. & Nesvizhskii, A.I. (2011) Abacus: a computational tool for extracting and pre-processing spectral count data for label-free quantitative proteomic analysis. *Proteomics*, **11**, 1340–1345.

Gandhi, A.K., Mendy, D., Waldman, M., Chen, G., Rychak, E., Miller, K., Gaidarova, S., Ren, Y., Wang, M., Breider, M., Carmel, G., Mahmoudi, A., Jackson, P., Abbasian, M., Cathers, B.E., Schafer, P.H., Daniel, T.O., Lopez-Girona, A., Thakurta, A. & Chopra, R. (2014) Measuring cereblon as a biomarker of response or resistance to lenalidomide and pomalidomide requires use of standardized reagents and understanding of gene complexity. *British Journal of Haematology*, **164**, 233–244.

Harousseau, J.L. & Moreau, P. (2009) Autologous hematopoietic stem-cell transplantation for multiple myeloma. *The New England Journal of Medicine*, **360**, 2645–2654.

Harousseau, J.L., Attal, M. & Avet-Loiseau, H. (2009) The role of complete response in multiple myeloma. *Blood*, **114**, 3139–3146.

Jakubowiak, A.J., Kendall, T., Al-Zoubi, A., Khaled, Y., Mineishi, S., Ahmed, A., Campagnaro, E., Brozo, C., Braun, T., Talpaz, M. & Kaminski, M.S. (2009) Phase II trial of combination therapy with bortezomib, pegylated liposomal doxorubicin, and dexamethasone in patients with newly diagnosed myeloma. *Journal of Clinical Oncology: Official Journal of the American Society of Clinical Oncology*, **27**, 5015–5022.

Jakubowiak, A.J., Dytfeld, D., Griffith, K.A., Lebovic, D., Vesole, D.H., Jagannath, S., Al-Zoubi, A., Anderson, T., Nordgren, B., Detweiler-Short, K., Stockerl-Goldstein, K., Ahmed, A., Jobkar, T., Durecki, D.E., McDonnell, K., Mietzel, M., Couriel, D., Kaminski, M. & Vij, R. (2012) A phase 1/2 study of carfilzomib in combination with lenalidomide and low-dose dexamethasone as a frontline treatment for multiple myeloma. *Blood*, **120**, 1801–1809.

Keshamouni, V.G., Michailidis, G., Grasso, C.S., Anthwal, S., Strahler, J.R., Walker, A., Arenberg, D.A., Reddy, R.C., Akulapalli, S., Thannickal, V.J., Standiford, T.J., Andrews, P.C. & Omenn, G.S. (2006) Differential protein expression profiling by iTRAQ-2DLC-MS/MS of lung cancer cells undergoing epithelial-mesenchymal transition reveals a migratory/invasive phenotype. *Journal of Proteome Research*, **5**, 1143–1154.

Khan, M.L., Reeder, C.B., Kumar, S.K., Lacy, M.Q., Reece, D.E., Dispenzieri, A., Gertz, M.A., Greipp, P., Hayman, S., Zeldenhurst, S., Dingli, D., Lust, J., Russell, S., Laumann, K.M., Mikhael, J.R., Leif Bergsagel, P., Fonseca, R., Vincent Rajkumar, S. & Keith Stewart, A. (2012) A comparison of lenalidomide/dexamethasone versus cyclophosphamide/lenalidomide/dexamethasone versus cyclophosphamide/bortezomib/dexamethasone in newly diagnosed multiple myeloma. *British Journal of Haematology*, **156**, 326–333.

Leung-Hagesteijn, C., Erdmann, N., Cheung, G., Keats, J.J., Stewart, A.K., Reece, D.E., Chung, K.C. & Tiedemann, R.E. (2013) Xbp1s-negative tumor B cells and pre-plasmablasts mediate therapeutic proteasome inhibitor resistance in multiple myeloma. *Cancer Cell*, **24**, 289–304.

Liang, S., Xu, Z., Xu, X., Zhao, X., Huang, C. & Wei, Y. (2012) Quantitative proteomics for cancer biomarker discovery. *Combinatorial Chemistry High Throughput Screening*, **15**, 221–231.

Lohr, J.G., Stojanov, P., Carter, S.L., Cruz-Gordillo, P., Lawrence, M.S., Auclair, D., Sougnez, C., Knoechel, B., Gould, J., Saksena, G., Cibulskis, K., McKenna, A., Chapman, M.A., Straussman, R., Levy, J., Perkins, L.M., Keats, J.J., Schumacher, S.E., Rosenberg, M., Multiple Myeloma Research, C., Getz, G. & Golub, T.R. (2014) Widespread genetic heterogeneity in multiple myeloma: implications for targeted therapy. *Cancer Cell*, **25**, 91–101.

Martinez-Lopez, J., Lahuerta, J.J., Pepin, F., Gonzalez, M., Barrio, S., Ayala, R., Puig, N., Montalban, M.A., Paiva, B., Weng, L., Jimenez, C., Sopena, M., Moorhead, M., Cedena, T., Rapado, I., Mateos, M.V., Rosinol, L., Oriol, A., Blanchard, M.J., Martinez, R., Blade, J., San Miguel, J., Faham, M. & Garcia-Sanz, R. (2014) Prognostic value of deep sequencing method for minimal residual disease detection in multiple myeloma. *Blood*, **123**, 3073–3079.

Mikhael, J.R., Dingli, D., Roy, V., Reeder, C.B., Buadi, F.K., Hayman, S.R., Dispenzieri, A., Fonseca, R., Sher, T., Kyle, R.A., Lin, Y., Russell, S.J., Kumar, S., Bergsagel, P.L., Zeldenrust, S.R., Leung, N., Drake, M.T., Kapoor, P., Ansell, S.M., Witzig, T.E., Lust, J.A., Dalton, R.J., Gertz, M.A., Stewart, K., Rajkumar, S.V., Chanan-Khan, A. & Lacy, M.Q. (2013) Management of newly diagnosed symptomatic multiple myeloma: updated Mayo Stratification of Myeloma and Risk-Adapted Therapy (mSMART) consensus guidelines 2013. *Mayo Clinic Proceedings*, **88**, 360–376.

Nicolas, E., Ramus, C., Berthier, S., Arlotto, M., Bouamrani, A., Lefebvre, C., Morel, F., Garin, J., Ifrah, N., Berger, F., Cahn, J.Y. & Mossuz, P. (2011) Expression of S100A8 in leukemic cells predicts poor survival in *de novo* AML patients. *Leukemia*, **25**, 57–65.

Obeng, E.A., Carlson, L.M., Gutman, D.M., Harrington, W.J. Jr, Lee, K.P. & Boise, L.H. (2006) Proteasome inhibitors induce a terminal unfolded protein response in multiple myeloma cells. *Blood*, **107**, 4907–4916.

Paiva, B., Gutierrez, N.C., Rosinol, L., Vidriales, M.B., Montalban, M.A., Martinez-Lopez, J., Mateos, M.V., Cibeira, M.T., Cordon, L., Oriol, A., Terol, M.J., Echeveste, M.A., de Paz, R., de Arriba, F., Palomera, L., de la Rubia, J., Diaz-Mediavilla, J., Sureda, A., Gorosquieta, A., Alegre, A., Martin, A., Hernandez, M.T., Lahuerta, J.J., Blade, J. & San Miguel, J.F. (2012) High-risk cytogenetics and persistent minimal residual disease by multiparameter flow cytometry predict unsustained complete response after autologous stem cell transplantation in multiple myeloma. *Blood*, **119**, 687–691.

Patel, V.J., Thalassinos, K., Slade, S.E., Connolly, J.B., Crombie, A., Murrell, J.C. & Scrivens, J.H. (2009) A comparison of labeling and label-free mass spectrometry-based proteomics approaches. *Journal of Proteome Research*, **8**, 3752–3759.

Pineda-Roman, M., Zangari, M., Haessler, J., Anaissie, E., Tricot, G., van Rhee, F., Crowley, J., Shaughnessy, J.D. Jr & Barlogie, B. (2008) Sustained complete remissions in multiple myeloma linked to bortezomib in total therapy 3: comparison with total therapy 2. *British Journal of Haematology*, **140**, 625–634.

Reece, D., Song, K.W., Fu, T., Roland, B., Chang, H., Horsman, D.E., Mansoor, A., Chen, C., Masih-Khan, E., Trieu, Y., Bruyere, H., Stewart, D.A. & Bahlis, N.J. (2009) Influence of cytogenetics in patients with relapsed or refractory multiple myeloma treated with lenalidomide plus dexamethasone: adverse effect of deletion 17p13. *Blood*, **114**, 522–525.

Richardson, P.G., Schlossman, R.L., Weller, E., Hideshima, T., Mitsiades, C., Davies, F., LeBlanc, R., Catley, L.P., Doss, D., Kelly, K., McKenney, M., Mechlowicz, J., Freeman, A., Deocampo, R., Rich, R., Ryoo, J.J., Chauhan, D., Balinski, K., Zeldis, J. & Anderson, K.C. (2002) Immunomodulatory drug CC-5013 overcomes drug resistance and is well tolerated in patients with relapsed multiple myeloma. *Blood*, **100**, 3063–3067.

Richardson, P.G., Sonneveld, P., Schuster, M.W., Irwin, D., Stadtmauer, E.A., Facon, T., Harousseau, J.L., Ben-Yehuda, D., Lonial, S., Goldschmidt, H., Reece, D., San-Miguel, J.F., Blade, J., Boccadoro, M., Cavenagh, J., Dalton, W.S., Boral, A.L., Esseltine, D.L., Porter, J.B., Schenkein, D. & Anderson, K.C. Assessment of Proteasome Inhibition for Extending Remissions I (2005). Bortezomib or high-dose dexamethasone for relapsed multiple myeloma. *The New England Journal of Medicine* **352**: 2487–2498.

Richardson, P.G., Weller, E., Lonial, S., Jakubowiak, A.J., Jagannath, S., Raje, N.S., Avigan, D.E., Xie, W., Ghobrial, I.M., Schlossman, R.L., Mazumder, A., Munshi, N.C., Vesole, D.H., Joyce, R., Kaufman, J.L., Doss, D., Warren, D.L., Lunde, L.E., Kaster, S., Delaney, C., Hideshima, T., Mitsiades, C.S., Knight, R., Esseltine, D.L. & Anderson, K.C. (2010) Lenalidomide, bortezomib, and dexamethasone combination therapy in patients with newly diagnosed multiple myeloma. *Blood*, **116**, 679–686.

Schewe, D.M. & Aguirre-Ghiso, J.A. (2009) Inhibition of eIF2alpha dephosphorylation maximizes bortezomib efficiency and eliminates quiescent multiple myeloma cells surviving proteasome inhibitor therapy. *Cancer Research*, **69**, 1545–1552.

Schwanhausser, B., Busse, D., Li, N., Dittmar, G., Schuchhardt, J., Wolf, J., Chen, W. & Selbach, M. (2011) Global quantification of mammalian gene expression control. *Nature*, **473**, 337–342.

Shilov, I.V., Seymour, S.L., Patel, A.A., Loboda, A., Tang, W.H., Keating, S.P., Hunter, C.L., Nuwaysir, L.M. & Schaeffer, D.A. (2007) The Paragon Algorithm, a next generation search engine that uses sequence temperature values and feature probabilities to identify peptides from tandem mass spectra. *Molecular & Cellular Proteomics: MCP*, **6**, 1638–1655.

Taguchi, F., Solomon, B., Gregorc, V., Roder, H., Gray, R., Kasahara, K., Nishio, M., Brahmer, J., Spreafico, A., Ludovini, V., Massion, P.P., Dziadziuszko, R., Schiller, J., Grigorieva, J., Tsypin, M., Hunsucker, S.W., Caprioli, R., Duncan, M.W., Hirsch, F.R., Bunn, P.A. Jr & Carbone, D.P. (2007) Mass spectrometry to classify non-small-cell lung cancer patients for clinical outcome after treatment with epidermal growth factor receptor tyrosine kinase inhibitors: a multicohort cross-institutional study. *Journal of the National Cancer Institute*, **99**, 838–846.

Ting, L., Cowley, M.J., Hoon, S.L., Guilhaus, M., Raftery, M.J. & Cavicchioli, R. (2009) Normalization and statistical analysis of quantitative proteomics data generated by metabolic labeling. *Molecular & Cellular Proteomics: MCP*, **8**, 2227–2242.

Unwin, R.D., Smith, D.L., Blinco, D., Wilson, C.L., Miller, C.J., Evans, C.A., Jaworska, E., Baldwin, S.A., Barnes, K., Pierce, A., Spooncer, E. & Whetton, A.D. (2006) Quantitative proteomics reveals posttranslational control as a regulatory factor in primary hematopoietic stem cells. *Blood*, **107**, 4687–4694.

Usaite, R., Wohlschlegel, J., Venable, J.D., Park, S.K., Nielsen, J., Olsson, L. & Yates Iii, J.R. (2008) Characterization of global yeast quantitative proteome data generated from the wild-type and glucose repression saccharomyces cerevisiae strains: the comparison of two quantitative methods. *Journal of Proteome Research*, **7**, 266–275.

Vellaichamy, A., Sreekumar, A., Strahler, J.R., Rajendiran, T., Yu, J., Varambally, S., Li, Y., Omenn, G.S., Chinnaiyan, A.M. & Nesvizhskii, A.I. (2009) Proteomic interrogation of androgen action in prostate cancer cells reveals roles of aminoacyl tRNA synthetases. *PLoS ONE*, **4**, e7075.

Vogel, C., Abreu Rde, S., Ko, D., Le, S.Y., Shapiro, B.A., Burns, S.C., Sandhu, D., Boutz, D.R., Marcotte, E.M. & Penalva, L.O. (2010) Sequence signatures and mRNA concentration can explain two-thirds of protein abundance variation in a human cell line. *Molecular Systems Biology*, **6**, 400.

Wang, H., Alvarez, S. & Hicks, L.M. (2012) Comprehensive comparison of iTRAQ and label-free LC-based quantitative proteomics approaches using two Chlamydomonas reinhardtii strains of interest for biofuels engineering. *Journal of Proteome Research*, **11**, 487–501.

Ward, P.S. & Thompson, C.B. (2012) Metabolic reprogramming: a cancer hallmark even warburg did not anticipate. *Cancer Cell*, **21**, 297–308.

Wong, T.W., Yu, H.Y., Kong, S.K., Fung, K.P. & Kwok, T.T. (2000) The decrease of mitochondrial NADH dehydrogenease and drug induced apoptosis in doxorubicin resistant A431 cells. *Life Sciences*, **67**, 1111–1118.

Zhang, X.-D., Baladandayuthapani, V., Lin, H.Y., Barlogie, B., Usmani, S.Z., Yang, L. & Orlowski, R.Z. (2013) Identification of Tight Junction Protein (TJP)-1 As a modulator and biomarker of proteasome inhibitor sensitivity in multiple myeloma. *Blood* (ASH Annual Meeting Abstracts), **122**, 123.

Zhou, Y., Barlogie, B. & Shaughnessy, J.D. Jr (2009) The molecular characterization and clinical management of multiple myeloma in the post-genome era. *Leukemia*, **23**, 1941–1956.

Zhu, Y.X., Braggio, E., Shi, C.X., Bruins, L.A., Schmidt, J.E., Van Wier, S., Chang, X.B., Bjorklund, C.C., Fonseca, R., Bergsagel, P.L., Orlowski, R.Z. & Stewart, A.K. (2011) Cereblon expression is required for the antimyeloma activity of lenalidomide and pomalidomide. *Blood*, **118**, 4771–4779.